Antiviral Research 172 (2019) 104637

Contents lists available at ScienceDirect

Antiviral Research

journal homepage: www.elsevier.com/locate/antiviral

Antiviral activity of the FDA-approved drug candesartan cilexetil against Zika virus infection

Marcus Wing Choy Loe[a], Regina Ching Hua Lee[a], Justin Jang Hann Chu[a,b,*]

[a] Laboratory of Molecular RNA Virology and Antiviral Strategies, Department of Microbiology and Immunology, Yong Loo Lin School of Medicine, National University Health System, National University of Singapore, MD4 Level 5, 5 Science Drive 2, Singapore, 117597, Singapore

[b] Institute of Molecular and Cell Biology, Agency for Science, Technology and Research (A*STAR), 61 Biopolis Drive, Proteos #06-05, 138673, Singapore

ARTICLE INFO

Keywords:
Zika
Antiviral
FDA-approved compounds
High-throughput screening

ABSTRACT

Zika virus (ZIKV) is a mosquito-borne virus that has risen to prominence as a significant threat to public health in the recent decade. Since its re-emergence in 2007, ZIKV has spread at an alarming rate and has since become endemic to multiple regions around the world. Infections are primarily asymptomatic, however the virus has become associated with the development of severe neurological complications such as Guillain–Barré syndrome (GBS) and congenital microcephaly. At present, there are currently no approved antivirals for ZIKV infections. In this study, we utilised a phenotype-based screening platform to perform a high-throughput screen on a 1172-compound US FDA-approved drug library to identify potential novel inhibitors against ZIKV. Candesartan cilexetil, an angiotensin II receptor inhibitor, displayed potent inhibition effects against ZIKV and subsequent downstream time-course studies revealed that it targets a post-entry stage(s) of the ZIKV replication cycle. Moreover, candesartan cilexetil also inhibited viral RNA production and viral protein synthesis. Candesartan cilexetil also exhibited antiviral effects against Dengue virus serotype-2 (DENV2), Kunjin virus (KUNV) and Chikungunya virus (CHIKV), indicating that its antiviral properties may not be restricted to ZIKV. Our study has demonstrated for the first time the potential application of candesartan cilexetil as an antiviral.

1. Introduction

The Zika virus (ZIKV) is an arthropod-borne virus that belongs to the genus *Flavivirus*; family *Flaviviridae* (Musso and Gubler, 2016). Other members of the family *Flaviviridae* include prominent human and animal pathogens such as dengue virus (DENV), Kunjin virus (KUNV), yellow fever virus and West Nile virus (Gould and Solomon, 2008). The virus was first isolated in a febrile rhesus monkey in 1947 in the Zika forest, Uganda (Dick, 1952), and subsequently in *Aedes africanus* mosquitoes in the same forest.

The first human ZIKV isolate was documented in Nigeria in 1954 (Musso and Gubler, 2016). Despite this, human ZIKV infections remained relatively sporadic and geographically widespread until 2007, when the first outbreak of ZIKV infection was reported on several islands in the State of Yap, Micronesia with an estimated 5000 cases of ZIKV (Musso et al., 2014). Subsequently by 2013, ZIKV was reported to have spread to other pacific islands, with outbreaks in French Polynesia, Easter Island, Cook Islands and Samoa (Song et al., 2017). The virus was first identified in the Americas in March 2015, in Bahia, Brazil, and was reported to have spread to 14 other states by October that year, with an estimated 1.3 million cases of ZIKV infection (Faye et al., 2014). To date, ZIKV has spread to more than 50 countries and territories, including Singapore, Thailand, Argentina, Mexico and the United States of America (World Health Organization, 2018) and has been declared a global health emergency by the World Health Organisation (WHO) in February 2016 (WHO, 2016).

ZIKV is primarily transmitted via vector-borne transmission, predominantly by the mosquito species *Aedes aegypti* and *Aedes albopictus* (Araujo et al., 2016; Ong, 2016). Aside from this, other forms of transmission have also been identified, namely sexual transmission and perinatal transmission from mother to fetus, in which the latter likely occurs due to viral crossing of the placenta or during delivery by viraemic mothers (Hamel et al., 2016). ZIKV infection may result in Zika fever. Majority of cases are asymptomatic and symptoms manifested, if any, are usually mild and self-limiting, such as fever, conjunctivitis, myalgia, headache, arthralgia and maculopapular rashes. ZIKV infections, however, have also been associated with severe neurological complications, such as Guillain–Barré syndrome (GBS),

* Corresponding author. Laboratory of Molecular RNA Virology and Antiviral Strategies, Department of Microbiology and Immunology, Yong Loo Lin School of Medicine, National University Health System, National University of Singapore, MD4 Level 5, 5 Science Drive 2, Singapore, 117597, Singapore.
E-mail address: miccjh@nus.edu.sg (J.J.H. Chu).

https://doi.org/10.1016/j.antiviral.2019.104637
Received 16 June 2019; Received in revised form 18 August 2019; Accepted 20 October 2019
Available online 25 October 2019

meningoencephalitis, myeletis and congenital microcephaly (Hayes, 2009; Fontes et al., 2016; Petersen et al., 2016). Despite its primarily asymptomatic and mild nature, the risks of long-term neurological complications enable ZIKV to pose a huge threat towards public health, particularly during outbreaks.

At present, there are no specific approved treatments or vaccines available against ZIKV. Primary strategies to combat infection are targeted at public health surveillance, vector control and prevention of ZIKV transmission (Hamel et al., 2016), and treatments administered are usually restricted to symptomatic relief (Saiz and Martin-Acebes, 2017). Previous studies, however, have identified compounds which exhibit antiviral properties against ZIKV *in vitro*. These include viral RNA-dependent RNA polymerase inhibitors such as sofosbuvir (Bullard-Feibelmann et al., 2017), pyramidine synthesis inhibitors such as finasteride, brequinar (Pascalino et al., 2016) and gemcitabine (Kuivanen et al., 2017), as well as compounds which can affect the pH-dependent steps of the viral replication cycle, namely saliphenylhalamide, obatoclax (Kuivanen et al., 2017) and niclosamide (Xu et al., 2016). ZIKV thus remains a prevalent threat to people living in mosquito-endemic regions. Due to the potential long-term consequences of ZIKV infection, there is an urgent need to develop potent and effective antiviral therapies to aid in the control of ZIKV outbreaks in the future.

To address the immediate need for the identification and development of antivirals against ZIKV, we performed an immunofluorescence-based high-throughput screen on a 1172-compound FDA-approved drug library utilising a phenotype-based screening platform previously developed by our laboratory to identify potential novel inhibitors of ZIKV. From the primary screen, a total of 29 compounds were identified as positive hits. Of these 29 compounds, candesartan cilexetil was selected for further investigation into its antiviral properties following downstream validation studies. Several downstream approaches were subsequently employed to elucidate its possible antiviral mechanism of action.

2. Materials and methods

2.1. Cell lines and viruses

Aedes albopictus larvae cells (C6/36; ATCC CRL-1660™), Baby Hamster Kidney fibroblasts (BHK-21) (ATCC CCL-10™), *Homo sapiens* placenta choriocarcinoma cells (JEG-3; ATCC HTB-36™), human cervix epithelial adenocarcinoma cells, (HeLa; ATCC CCL-2™), human kidney embryonic cells (HEK293T; ATCC CRL-11268 ™), human hepatoma cells (Huh7; Dr Priscilla Yang, Harvard Medical School, USA), human muscle rhabdomyosarcoma cells (RD; ATCC CCL-136™), human umbilical vein endothelial cells (HUVEC; ATCC CRL-1730™) and African green monkey kidney cells (Vero, ATCC CCL-81™) were utilised in this study. C6/36 cells were cultured in Leibovitz-15 (L-15) medium (Sigma-Aldrich) supplemented with 10% heat-inactivated fetal calf serum (HI-FCS; Capricorn Scientific) and maintained at 28 °C in the absence of carbon dioxide (CO_2). BHK-21 cells were cultured in Roswell Park Memorial Institute 1640 medium (RPMI-1640; Sigma-Aldrich) supplemented with 10% fetal calf serum (FCS), whereas JEG-3, HeLa, HEK293T, Huh7, Vero and RD cells were cultured in Dulbecco's Modified Eagle's Medium (DMEM) (Sigma-Aldrich) supplemented with 10% HI-FCS. Both types of media were buffered with 2 g sodium hydrogen carbonate, and all six cell lines were maintained at 37 °C, 5% CO_2. HUVEC cells were maintained in Endothelial Cell Growth Basal Medium-2 (EBM-2, Lonza). Five different viruses were used in this study, which are ZIKV PRVABC59 strain (GenBank accession no. KU501215.1), DENV2 New Guinea C (NGC) strain (GenBank accession no. KM204118.1), Chikungunya virus (CHIKV) SGEHICHD122508 strain (GenBank accession no. FJ445502.2), Enterovirus 71 (EV-A71) strain 41 (GenBank accession no. AF316321.2) and Kunjin virus (KUNV) MRM61C strain. ZIKV, DENV2, and CHIKV were propagated in C6/36 cells, whereas EV-A71 and KUNV were propagated in RD and Vero cells respectively.

2.2. FDA-approved drug library

The primary screen to identify novel compounds with potential antiviral effects against ZIKV infection was performed on a 1172-compound FDA-approved drug library (Selleckchem). The complete list of compounds present in an updated version of the library can be found at https://www.selleckchem.com/screening/fda-approved-drug-library.html. Compounds were first dissolved in 100% dimethyl sulfoxide (DMSO) to obtain a concentration of 10 mM, following which the compounds were further diluted in serum-free media to obtain a concentration of 100 μM and stored at −20 °C until use.

2.3. Primary screen

JEG-3 cells were seeded on 96-well plates (Corning) at a seeding density of 1.3×10^5 cells per mL and incubated at 37 °C, 5% CO_2 overnight. Cells were infected with ZIKV at a Multiplicity of Infection (MOI) of 5 and incubated for 1 h at 37 °C, 5% CO_2 with gentle rocking every 15 min. Compounds from the library were subsequently added to ZIKV-infected cells at a final concentration of 10 μM and the plates incubated for a further 24 h at 37 °C, 5% CO_2. ZIKV-infected cells treated with 0.1% DMSO and 80 μM ribavirin served as vehicle and positive controls respectively. After incubation, the cell monolayer was fixed with −20 °C methanol (Sinopharm Chemical), following which the cells were washed thrice with 100 μL of 1 x Phosphate Buffer Saline (PBS) and subsequently rehydrated in 50 μL of 1 x PBS. Indirect immunofluorescence assay was then performed. The cells were first incubated with ZIKV Anti-E-protein DIII ZV-67 (Absolute Antibody) 1° antibody at a 1:100 dilution at 37 °C for 1 h, following which the cells were washed and incubated with anti-rabbit fluorescein isothiocyanate (FITC, Merck Millipore) 2° antibody at a 1:200 dilution at 37 °C for another hour. After incubation, the cells were washed and subsequently incubated with DAPI (Sigma-Aldrich) for 15 min at room temperature. Following which, cells were washed and stored in 50 μL of 1 x PBS.

2.4. Data acquisition

The stained cells were viewed via the Operetta High-Content Imaging System, using the Harmony High-Content Imaging and Analysis Software (PerkinElmer). Images were taken at 10× magnification of a central pre-defined region of each well using both DAPI and fluorescein channels and subsequently analysed with the Cell Profiler software (Carpenter et al., 2006). The total number of cells for each well was determined by the count obtained for the DAPI-stained nuclei, whereas the total number of ZIKV-infected cells was determined by the count obtained for the FITC-stained cytoplasm. Percentage infection for each well was calculated via the formula $\frac{ZIKV - infected\ cell\ count}{Total\ cell\ count}$ x 100%. Percentage inhibition was then subsequently determined using the formula $\frac{PI_V - PI_T}{PI_V}$ x 100%, where PI_V represents the percentage infection of vehicle control treated ZIKV infected wells i.e. ZIKV infected wells treated with 0.1% dimethyl sulfoxide (DMSO), and PI_T represents the percentage infection of FDA-library drug treated ZIKV infected wells. Compounds that presented a percentage inhibition value of 50% or greater relative to the 0.1% DMSO-treated controls were identified as positive hits. From the list of primary hits, a number of compounds were subsequently selected for further validation of their antiviral properties against ZIKV.

The robustness of the phenotype-based screening platform utilised for the primary screen was determined using the Z-factor, a statistical parameter that serves as an indication of the capability and fidelity of the platform in terms of hit identification. To determine the Z-factor, JEG-3 cells were seeded in 96-well plates and incubated overnight. Of the 96 wells, 48 were infected with ZIKV at MOI 5, whereas the

remaining 48 were mock-infected with DMEM media supplemented with 2% HI-FCS and incubated for 1 h. After which, the cells were washed twice with 100 µL of 1 x PBS and incubated with DMEM, 2% HI-FCS at 37 °C with 5% CO_2 for 24 h. After incubation, the cells were fixed and indirect immunofluorescence assay was performed. Images of each well were taken and the percentage infection determined as per the methods described above. The Z-factor of the screening platform was derived using the formula $\left(1 - \frac{3(\sigma_p + \sigma_n)}{|\mu_p - \mu_n|}\right)$ x 100%, where µ and σ represent the mean and standard deviation of the percentage infection respectively, and p and n represent the positive (ZIKV-infected) and negative (mock-infected) controls respectively (Zhang et al., 1999).

2.5. Validation of primary hits

Hits identified from the primary screen were validated using cell viability and dose-dependent inhibition assays. To determine the cell viability profiles of each compound, JEG-3 cells were seeded on 96-well plates and incubated overnight at 37 °C, 5% CO_2. Cells were treated with the compounds at varying concentrations and incubated for a further 24 h at 37 °C, 5% CO_2. 0.1% DMSO was utilised as the vehicle control. After 24 h, the media was removed, alamarBlue Cell Viability Reagent (Thermo Fisher Scientific) diluted in DMEM, 2% HI-FCS in a 1:10 dilution factor was added to each well and the cells incubated for 2.5 h. Fluorescence measurements for each well were obtained via the Infinite™ 200 series microplate reader (Tecan), at emission and excitation wavelengths of 585 nm and 570 nm respectively and the cell viabilities subsequently determined. Measurements obtain from compound-treated or 0.1% DMSO-treated cells were normalised against those obtained from non-treated cells to obtain the relative cell viability.

Validation of the primary hits identified were performed via dose-dependent inhibition assays. JEG-3 cells were seeded on 24-well plates (Greiner Bio-One) at a seeding density of 7×10^4 cells per mL and incubated at 37 °C, 5% CO_2 overnight. Cells were then infected with ZIKV at MOI 5 and incubated for 1 h at 37 °C, 5% CO_2. After incubation, the cells were washed twice with 1 mL 1 x PBS, followed by treatment with varying concentrations of each drug diluted in DMEM, 2% HI-FCS. The cells were incubated for a further 24 h at 37 °C with 5% CO_2, following which the supernatant was harvested and viral titres determined via plaque assay.

2.6. Viral plaque assays

Viral titres were quantified via viral plaque assays. For plaque assays involving ZIKV, DENV2, CHIKV and KUNV, BHK-21 cells were seeded on 24-well plates and incubated at 37 °C with 5% CO_2 overnight. Supernatants harvested from virus-infected samples were subjected to a 10-fold serial dilutions in RPMI-1640 media supplemented with 2% FCS. BHK-21 cells were infected with 100 µL of diluted virus suspension and incubated for 1 h at 37 °C with 5% CO_2. After infection, BHK-21 cells were washed twice with 1 mL of 1 x PBS, followed by the addition of 1% carboxymethyl-cellulose (CMC) containing RPMI-1640 and 2% FCS. The cells were then incubated for 3 (KUNV, CHIKV), 4 (ZIKV) or 6 (DENV2) days at 37 °C with 5% CO_2. After incubation, the cells were fixed and stained with 4% paraformaldehyde (PFA) and 1% crystal violet. Viral plaques were counted and the viral titre was subsequently quantified in PFU/mL.

For plaque assays involving EV-A71, RD cells were seeded on 24-well plates at a seeding density of 2×10^5 cells/mL and incubated at 37 °C with 5% CO_2 overnight. Supernatants harvested from virus-infected samples were subjected to a 10-fold serial dilutions in DMEM media supplemented with 2% FCS. RD cells were infected with 100 µL of diluted virus suspension and incubated for 1 h at 37 °C with 5% CO_2. After infection, RD cells were washed twice with 1 mL of 1 x PBS, followed by the addition of 0.5% agarose (Vivantis) containing DMEM and 2% FCS. The cells were then incubated for 4 days at 37 °C with 5% CO_2. After incubation, the cells were fixed and stained with 4% paraformaldehyde (PFA) and 1% crystal violet. Viral plaques were counted and the viral titre was subsequently quantified in PFU/mL.

2.7. Time-of-addition and time-of-removal studies

For both time-of-addition and time-of removal studies, JEG-3 cells were seeded on a 96-well plate, incubated overnight and infected with ZIKV at MOI 5. After a 1 h at 37 °C, 5% CO_2, the cells were washed once with 1 x PBS. For the time-of-addition study, DMEM, 2% HI-FCS was subsequently added at 0 h post infection (hpi). At time-points of 0, 2, 4, 6, 8, 12, 18 hpi, media was removed and the ZIKV-infected cells treated with 5 µM candesartan cilexetil. For the time-of-removal assay, the cells were treated with 5 µM candesartan cilexetil at 0 hpi. At time-points of 0, 2, 4, 6, 8, 12, 18 hpi, the compound was removed and replaced with DMEM, 2% HI-FCS. All supernatants were harvested at 24 hpi and viral titres quantified via plaque assay.

2.8. Pre-treatment, Co-treatment and entry bypass studies

In all three studies, JEG-3 cells were first seeded on 24-well plates and incubated at 37 °C, 5% CO_2 overnight. For the pre-treatment study, JEG-3 cells were first treated with 5 µM candesartan cilexetil for 2 h at 37 °C, 5% CO_2, following which the cells were washed twice with 1 x PBS. Cells were then infected with ZIKV at MOI 5 and incubated for 1 h at 37 °C, 5% CO_2. After which, the cells were washed twice with 1 x PBS and subsequently incubated in DMEM, 2% HI-FCS for 24 h.

The co-treatment study was performed by first treating ZIKV at MOI 5 with 5 µM candesartan cilexetil and incubated for 30 min at 37 °C. Following which, the viruses were subjected to centrifugal filtration using a 100,000-molecular-weight centrifugal filter unit (Sartorius) at $1500 \times g$ for 5 min at 4 °C to remove the excess unbound drug molecules. The viruses were then re-suspended in 1 mL of 1 x PBS and filtered through the same filter units at $1500 \times g$ for 5 min at 4 °C before being re-suspended in DMEM, 2% HI-FCS to obtain the original concentration of ZIKV. The purified virus was then used to infect JEG-3 cells and incubated for 1 h. After which, the cells were washed twice with 1 x PBS and subsequently incubated in DMEM, 2% HI-FCS for 24 h.

For the entry bypass studies, ZIKV viral RNA was first extracted via the QIAamp Viral RNA Mini Kit (QIAGEN) according to the manufacturer's protocol. JEG-3 cells were transfected with 500 ng of ZIKV viral RNA and subsequently treated with 5 µM candesartan cilexetil for 24 h. During transfection, 500 ng of ZIKV viral RNA and 1 µL Lipofectamine 2000 (Thermo Fisher Scientific) were diluted in 50 µL serum-free DMEM respectively at room temperature for 5 min. Both solutions were subsequently mixed and incubated for a further 30 min at room temperature to allow for formation of complexes. 100 µL of ZIKV RNA-Lipofectamine 2000 complexes was then added to JEG-3 cells and incubated for 1 h at 37 °C, 5% CO_2 to allow for transfection to occur. Following incubation, candesartan cilexetil diluted in DMEM, 2% HI-FCS was added to the wells to obtain a final concentration of 5 µM and incubated for 48 h 37 °C, 5% CO_2. JEG-3 cells and ZIKV treated with 0.1% DMSO served as controls for all three studies. All supernatants were harvested and viral titres quantified via plaque assay.

2.9. Quantitative reverse transcription-polymerase chain reaction (qRT-PCR)

For sample preparation for qRT-PCR, JEG-3 cells were first seeded on 24-well plates and incubated at 37 °C, 5% CO_2 overnight. Cells were then infected with ZIKV at MOI 5, incubated for 1 h at 37 °C, 5% CO_2, following which the cells were washed twice with 1 x PBS and treated with 5 µM candesartan cilexetil. ZIKV-infected cells treated with 0.1% DMSO and 5 µM emetine served as the vehicle and positive controls

respectively. At 14 hpi, total RNA was extracted via the RNeasy Mini Kit (QIAGEN) in accordance with the manufacturer's protocol.

Reverse transcription was first carried out to generate the cDNA of both the positive- and negative-sense ZIKV viral RNA. A 25 μL reaction mixture containing 11 μL of nuclease-free water, 5 μL of MMLV 5X Reaction Buffer (Promega), 1 μL of 200 units of M-MLV reverse transcriptase (Promega), 1 μL of dNTP mix, 1 μL of either the forward or reverse primer (10 μM), and 6 μL of viral RNA was prepared for each sample and reverse transcription was performed at 42 °C for 30 min. Following which, qPCR was carried out to induce the synthesis of the second strand, amplification and quantification of the viral cDNA. For each sample, a 20 μL reaction mixture containing 7 μL of nuclease-free water, 10 μL of PrimeTime™ Gene Expression Master Mix (IDT), 0.5 μL forward and reverse primers, 0.5 μL of pan-ZIKV-1 probe and 1 μL of the cDNA was prepared. The qPCR reaction was subsequently conducted with the following steps: polymerase activation at 95 °C for 2 min and 40 cycles of PCR (denaturation for 15 s at 95 °C and annealing and extension at 60 °C for 60 s) in the Applied Biosystems StepOnePlus real-time PCR system (Applied Biosystems). Cycle threshold values for each sample was obtained and normalised using the β-actin gene, which served as the endogenous control. Quantification of the β-actin mRNA was done via qRT-PCR using the same parameters as above. The absolute ZIKV positive- and negative-sense viral RNA copy numbers were subsequently derived from the cycle threshold values via the use of a standard curve as a reference. ZIKV primer sequences utilised for this study are indicated as follows: 5′-GAGTGTGATCCAGCCGTTATT-3'; reverse, 5′-CAGCCTCCATGTGTCATTCT-3'.

2.10. SDS-PAGE and western blot

Western blot samples were prepared by first seeding JEG-3 cells on 24-well plates and incubated at 37 °C, 5% CO_2 overnight. Cells were then infected with ZIKV at MOI 5, incubated for 1 h at 37 °C, 5% CO_2, following which the cells were washed twice with 1 x PBS and treated with 5 μM candesartan cilexetil. At 14 hpi, cells were lysed with 1 x Laemmli SDS-PAGE buffer and the wells scraped to obtain the cell lysate. Proten-containing samples were first separated via SDS-PAGE using 10% acrylamide gels that were ran at for 2.5 h at 100 V. The PageRuler prestained protein ladder (Fermentas) was utilised as a molecular weight standard. Separated proteins on the gels were subsequently transferred to a polyvinylidene difluoride (PVDF) membrane via the Bio-Rad semidry transfer system (Bio-Rad) at 1.3A for 10 min.

Detection of the ZIKV envelope protein was then carried out. The PVDF membrane was first blocked with 5% skim milk dissolved in Tris-buffered saline-Tween 20 (TBST) for 1 h. After blocking, ZIKV Anti-E-protein DIII ZV-67 (Absolute Antibody) 1° antibody at a dilution factor of 1:500 was added and the membrane incubated overnight. The membrane was then washed thrice with TBST for 5 min, followed by the addition of the 2° antibody, polyclonal goat anti-rabbit IgG (H + L) horseradish peroxidase (Thermo Fisher Scientific) at a dilution factor of 1: 5000 and subsequently incubated for 1 h. The membrane was subsequently washed three times with TBST and developed with the enhanced chemiluminescence (ECL) method via the SuperSignal West Pico chemiluminescent substrate (Thermo Fisher Scientific.

The loading control, β-actin, was detected via a similar method. After blocking, the anti-β-actin mouse monoclonal 1° antibody (Merck-Millipore) and the AP-conjugated goat anti-mouse IgG 2° antibody (Thermo Fisher Scientific) at a dilution factor of 1: 20000 was then added and the membrane incubated for 30 min. The membrane was subsequently washed three times and developed using the ECL method as mentioned above.

2.11. Antiviral activity of candesartan cilexetil against other viruses

The potential antiviral properties of candesartan cilexetil were also investigated against other viruses, namely DENV2, KUNV, CHIKV and EV-A71. Cell viability assays were first performed to determine the concentration range at which candesartan cilexetil is non-cytotoxic in various cell lines via the use of the alamarBlue Cell Viability Reagent, as mentioned above. Following which, dose-dependent inhibition assays were performed to evaluate the inhibitory effects of candesartan cilexetil against each virus. All supernatants were harvested and viral titres quantified via plaque assays. The table below indicates the cell line, seeding densities used for both 24- and 96-well plate formats, MOI and incubation time utilised for assays involving the four viruses.

Virus	Cell Line	Seeding density (96-well plate)/ cells/mL	Seeding density (24-well plate)/ cells/mL	MOI	Incubation time/hours
DENV2	HEK293T	2×10^5	1×10^5	1	48
KUNV	HEK293T	2×10^5	1×10^5	1	48
CHIKV	HeLa	7×10^4	9×10^4	1	48
EV-A71	RD	2×10^5	1×10^5	1	12

2.12. Statistical analyses

One-way analysis of variance (ANOVA) was utilised to determine the statistical significance of data obtained. Samples that expressed statistical difference when compared to the control values (p-values obtained < 0.05, 0.01 and 0.001) were then subjected to a Dunnett's post-test. The two-tailed students' T-test was also utilised to evaluate the significance of data involving the comparison of two different samples.

3. Results

3.1. Establishment of the phenotype-based screening platform

The phenotype-based screening platform used in this study was previously developed by our laboratory for high-throughput screening of potential antivirals against ZIKV infection (Lee et al., 2019). It utilises an immunofluorescence-based approach to detect the ZIKV viral envelope protein, which functions as an indicator of ZIKV infection and replication. To further ascertain its reliability for use in this study, the Z-factor of the screening assay was evaluated. This was done by infecting 48 wells of JEG-3 cells with ZIKV at MOI 5 and mock-infecting another 48 wells of JEG-3 cells with DMEM medium, 2% FCS, after which indirect immunofluorescence assay was performed and the infection rate of each well determined. Fig. 1 represents the percentage infections determined for the mock-infected and ZIKV-infected wells. A distinct separation was observed in terms of percentage infection between the two groups, and subsequently a Z-factor of 0.529 was obtained, indicating that the platform is suitable for use in high-throughput screening (Zhang et al., 1999).

3.2. Primary screen

Following the establishment of the phenotype-based screening platform, a primary screen was performed on a 1172-compound FDA-approved drug library (Selleckchem) to identify potential compounds that express antiviral properties against ZIKV infection. Compounds were screened at a concentration of 10 μM and the percentage inhibition of each compound against ZIKV infection relative to the control, 0.1% DMSO was determined. Ribavirin, a compound previously reported to exhibit antiviral properties against ZIKV infection both *in vitro* and in vivo (Kamiyama et al., 2017) was used as a positive control, at a concentration of 80 μM. Compounds that exhibited ≥50% inhibition of ZIKV infection were identified as positive hits (Table S1).

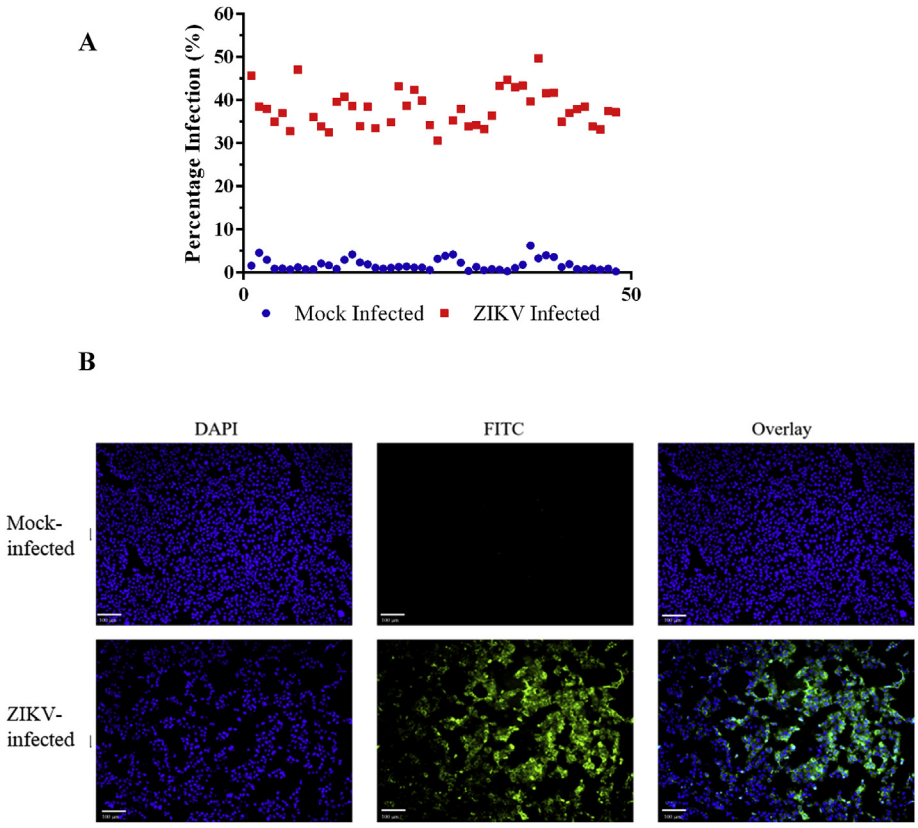

Fig. 1. Determination of Z-factor of the phenotype-based screening platform A) Scatter plot representing the percentage infection of mock-infected and ZIKV-infected data points. 48 individual data points were used for mock-infected and ZIKV-infected respectively. The Z-factor was evaluated to be 0.529, indicating that the screening assay is robust and suitable for use in high-throughput screens. B) Representative indirect immunofluorescence images of mock-infected and ZIKV-infected JEG-3 cells (MOI 5) at 10× magnification obtained.

3.3. Candesartan cilexetil is a novel, potent inhibitor of ZIKV infection

From the list of 29 compounds identified as positive hits, four compounds were subsequently chosen for further evaluation of their potential antiviral properties against ZIKV, namely candesartan cilexetil, emetine, primaquine diphosphate and calcifediol. These compounds included a mixture of compounds with previously reported antiviral effects against flaviviruses, such as emetine, as well as compounds with no known antiviral properties, such as candesartan cilexetil and calcifediol.

Dose-dependent inhibition studies were performed for all five compounds to evaluate their respective inhibitory effects against ZIKV, and viral plaque assays were used to quantify viral titres. Additionally, cell viability assays were also performed using the alamarBlue Cell Viability Reagent to ascertain that any inhibitory effects on ZIKV infection observed were not due to cytotoxic effects as a result of drug treatment.

All four compounds that were evaluated exhibited inhibitory effects against ZIKV infection (Fig. 2A–D). Calcifediol and candesartan cilexetil displayed dose-dependent inhibition against ZIKV infection, with a 4.8 and 4.4 $\log_{10}$ fold decrease in viral titres respectively at 10 μM. Emetine displayed a 4.0 $\log_{10}$ fold decrease in viral titre at 5 μM. Treatment with primaquine diphosphate resulted in a 1 $\log_{10}$ fold decrease in viral titre 0.5 μM, however the inhibitory effect was observe to plateau even at higher concentrations. Cell viability remained close to or above 80% for all concentrations of each compound that was assayed, indicating that the antiviral effects observed were unlikely to be due to cytotoxic effects caused by the presence of the compounds. The 50% cytotoxic concentration (CC_{50}) and the 50% inhibitory concentration (IC_{50}) values were derived from the cell viability and dose-dependent inhibition studies respectively and were subsequently used to derive the selectivity index (SI) value for each compound (Table 1).

Despite the observed antiviral effects against ZIKV for all four drugs that were identified, candesartan cilexetil was subsequently selected for further downstream analysis of its anti-ZIKV properties due to its significant inhibition of ZIKV infection, relatively more favourable selectivity index profile and its novel status as an antiviral against ZIKV.

3.4. Candesartan cilexetil exhibits antiviral effects against ZIKV in a various cell lines

The antiviral effects of candesartan cilexetil were also evaluated in various other cell lines, namely baby hamster kidney fibroblasts BHK-21, HEK293T and Huh7 cells. HUVEC cells, a primary cell line, was also utilised. The dose-dependent inhibitory effect of candesartan cilexetil was recapitulated in ZIKV-infected HUVEC and HEK293T cells, albeit at a decreased potency relative to drug treatment on ZIKV-infected JEG-3 cells (Fig. 3A and B), whereas no antiviral effects against ZIKV were observed in BHK-21 and Huh7 cells (Fig. 3C and D) This difference in susceptibility to candesartan cilexetil treatment could potentially be attributed to its mechanism of action, suggesting that there may some specificity involved in the components targeted by the drug which differ amongst various cell lines (Van Der Hoek et al., 2017).

3.5. Candesartan cilexetil inhibits a post-entry stage of the ZIKV replication cycle

Time-of-addition and time-of-removal studies were first performed to determine the window in the ZIKV replication cycle candesartan cilexetil likely exerts its antiviral effects on. Following ZIKV infection and incubation, 5 μM candesartan cilexetil was introduced at specific intervals (0, 2, 4, 6, 8, 12 & 18 hpi) for the time-of-addition assay, whereas for the time-of-removal assay, the compound was added at 0 hpi and removed at specific intervals (Fig. 4A). ZIKV-infected cells treated with the vehicle control, 0.1% DMSO, served as controls for each assay (Fig. 4B). Supernatants were subsequently harvested at 24 hpi, and viral titres were quantified. Gradual declines in viral titres were observed for both time-of-addition and time-of-removal assays as

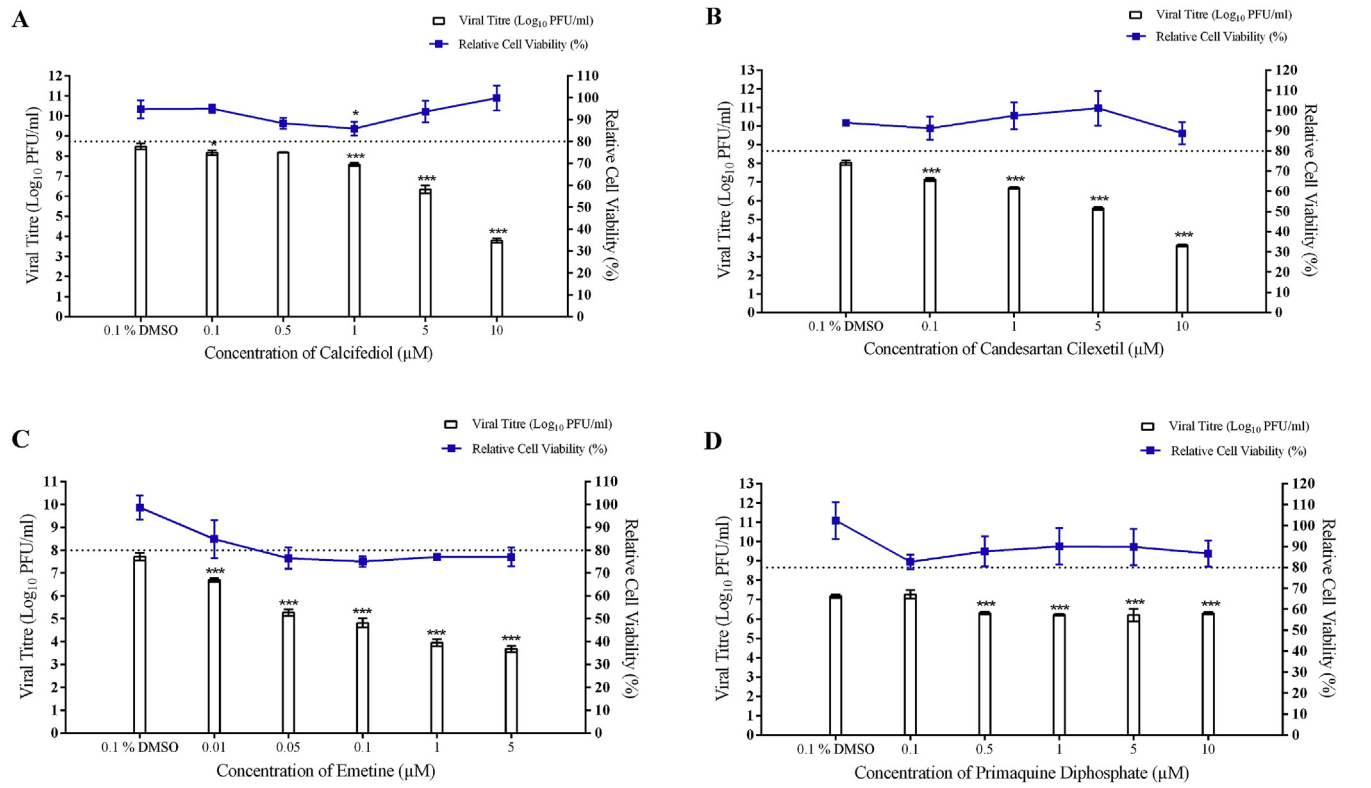

Fig. 2. Validation of secondary hits in JEG-3 cells via cell viability and dose-dependent inhibition of anti-ZIKV activity. JEG-3 cells were infected with ZIKV at MOI 5 and treated with A) calcifediol, B) candesartan cilexetil, C) emetine and D) primaquine diphosphate at various concentrations. Antiviral properties against ZIKV were observed for all four compounds. The primary axis corresponds to the viral titre observed, whereas the secondary axis corresponds to the relative cell viability. Dashed line indicates the CC_{20} cut-off for cell viability. One-way ANOVA and Dunnett's post-test were utilised to determine the presence of any statistical difference, with * denoting that $P < 0.05$, and *** denoting that $P < 0.001$. Error bars represent the standard deviation observed from the means of triplicates performed for both cell viability and dose-dependent inhibition studies.

Table 1
CC_{50}, IC_{50}, and SI values of secondary hits, derived from data obtained from cell viability and dose-dependent inhibition assays respectively. All five drugs were observed to possess antiviral properties against ZIKV.

No.	Drug	CC_{50} (μM)	IC_{50} (μM)	Selectivity Index (SI)
1	Primaquine Diphosphate	> 100	0.1605	> 623.0530
2	Emetine	–	0.00411	–
3	Calcifediol	26.27	0.02215	1186.0045
4	Candesartan Cilexetil	22.33	0.003363	6639.9048

the interval between infection and addition or removal increased, with the exception of a significant increase when the compound was added at 18 hpi, as compared to 12 hpi, in the time-of-addition curve. The two curves intersect at 15.3 hpi, suggesting that candesartan cilexetil exerts its antiviral effect on a post-entry stage(s) of the viral replication cycle.

Pre-treatment studies were utilised to determine if candesartan cilexetil is able to inhibit ZIKV entry into host cells by either affecting the surface of the host cell such that it prevents the virus from binding or by interfering with the viral entry via receptor-mediated endocytosis. This was done by first treating JEG-3 cells with 5 μM candesartan cilexetil for 2 h prior to infection. As seen in Fig. 5A, minimal differences in viral titre were observed between cells treated with candesartan cilexetil and cells treated with the vehicle control, 0.1% DMSO, suggesting that candesartan cilexetil is unlikely to inhibit ZIKV entry into host cells.

Co-treatment studies were also performed to complement data obtained from the pre-treatment, time-of-addition and time-of-removal studies to investigate if candesartan cilexetil is capable of interacting with the surface proteins of the viral particle, preventing it from binding to the host cell. ZIKV was first treated with 5 μM candesartan cilexetil for 30 min, before being subjected to centrifugal filtration to facilitate removal of excess compound, after which the virus was used to infect JEG-3 cells. Co-treatment with candesartan cilexetil also failed to yield any significant decrease in viral titre (Fig. 5B), further supporting the previous observations that candesartan cilexetil acts on a post-entry event(s) and is unlikely to affect viral binding or entry into host cells.

Entry bypass studies were subsequently carried out to further verify that the antiviral effects of candesartan cilexetil occur at a post-entry event(s) by transfecting JEG-3 cells with ZIKV genomic RNA and treating the cells with 5 μM candesartan cilexetil. Transfection of the cells with viral RNA bypasses the early stages of the replication cycle, namely the viral entry, uncoating and release of viral RNA into the host cytoplasm, allowing for the exclusion of these processes from the replication cycle. Following treatment with candesartan cilexetil, a significant decrease in viral titre was observed (Fig. 5C), indicating that the compound is still able to exert its antiviral effects and further parallels the observations made from the previous studies that candesartan cilexetil does not inhibit the viral binding and entry stages of the ZIKV replication cycle.

3.6. Candesartan cilexetil inhibits ZIKV RNA replication and ZIKV protein synthesis

Having previously established that candesartan cilexetil likely targets a post entry stage(s) of the ZIKV replication cycle, its effect on viral RNA replication and protein synthesis was further investigated via qRT-PCR and western blot analyses respectively. qRT-PCR was performed on ZIKV-infected JEG-3 cells treated with 5 μM candesartan cilexetil for 14 h. ZIKV-infected cells treated with 0.1% DMSO and 5 μM emetine, a

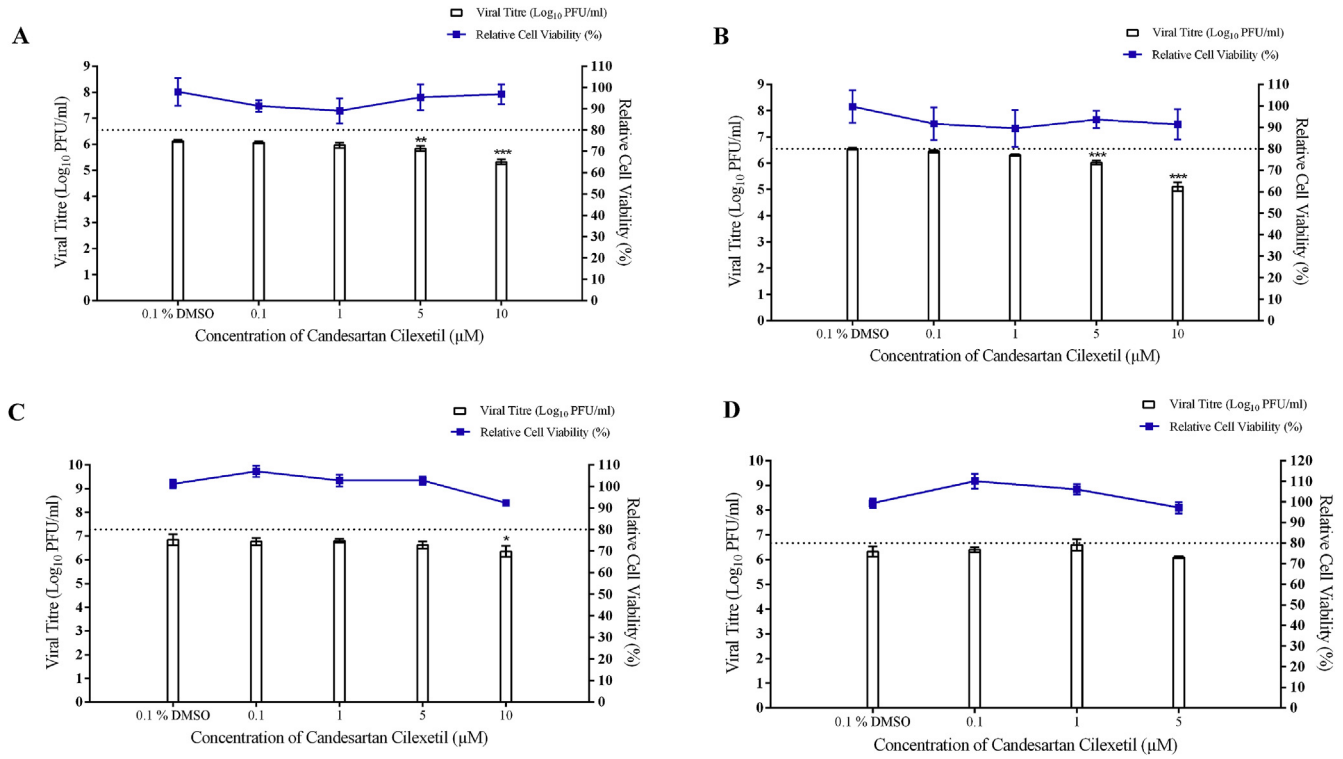

Fig. 3. Antiviral effects of candesartan cilexetil on ZIKV infection in other cell lines. A) HUVEC, B) HEK293T cells C) BHK-21 and D) Huh7 cells were infected with ZIKV at MOI 5 and treated with candesartan cilexetil at various concentrations. Antiviral effects were observed against ZIKV upon treatment with candesartan cilexetil. The primary axis corresponds to the viral titre observed, whereas the secondary axis corresponds to the relative cell viability. Dashed line indicates the CC_{20} cut-off for cell viability. One-way ANOVA and Dunnett's post-test were utilised to determine the presence of any statistical difference, with * denoting that $P < 0.05$, and *** denoting that $P < 0.001$. Error bars represent the standard deviation observed from the means of triplicates performed for both cell viability and dose-dependent inhibition studies.

compound previously report to be able to affect flavivirus RNA replication (Low et al., 2009), served as the vehicle and positive controls respectively. Following qRT-PCR, the cycle threshold values of each sample was obtained, normalised against their respective β-actin levels and subsequently converted into viral RNA copy numbers, utilising a standard curve as reference. The results obtained show that significant decreases in viral RNA copy numbers for both positive- and negative-sense strands were observed after treatment with 5 μM candesartan cilexetil (Fig. 6A), which suggests that the compound may exert an inhibitory effect on ZIKV viral RNA synthesis.

Western blot analyses were subsequently carried out to determine the effect of candesartan cilexetil on ZIKV viral protein synthesis. It was observed that treatment of ZIKV-infected cells with 5 μM candesartan cilexetil resulted in a significant reduction in ZIKV envelope protein detected, relative to ZIKV-infected cells that were treated with the vehicle control, 0.1% DMSO (Fig. 7B and C), suggesting that candesartan cilexetil is able to affect viral protein synthesis. β-Actin served as a loading control, and also to ensure that the synthesis and expression of host cell proteins were unaffected by the concentration of candesartan cilexetil administered.

Further evaluation was performed to determine if the reduction in viral protein expression due to candesartan cilexetil treatment was mediated via accelerated proteolysis of the viral proteins. To evaluate this, MG132, a proteosome inhibitor was utilised. Treatment with a combination of MG132 and candesartan cilexetil failed to induce a rescue effect in the ZIKV envelope protein level (Fig. 7A and B), indicating that the decrease in viral protein expression observed was unlikely to be mediated by accelerated proteolysis via host proteosomes. β-Actin served as a loading control, and also to ensure that the synthesis and expression of host cell proteins were unaffected by the concentration of candesartan cilexetil administered.

3.7. Candesartan cilexetil exhibits broad-spectrum antiviral effects against DENV2, KUNV and CHIKV

The potential broad-spectrum antiviral properties of candesartan cilexetil were investigated via dose-dependent inhibition studies performed on other viruses, namely DENV2, KUNV, CHIKV and EV-A71. Candesartan cilexetil was shown to also inhibit DENV2 and KUNV (Fig. 8A and B), which like ZIKV, are flaviviruses, at non-cytotoxic concentrations. Interestingly, candesartan cilexetil also demonstrated inhibitory effects against CHIKV (Fig. 8C), an alphavirus, whilst not exhibiting any antiviral effects against EV-A71 (Fig. 8D). This suggests that the antiviral activity of candesartan cilexetil may not be restricted to flaviviruses, and could potentially extend to other RNA viruses as well. The respective IC_{50} values derived for candesartan cilexetil treatment against each virus is presented in Table 2.

4. Discussion

Despite its predominantly asymptomatic and mild nature, ZIKV has been associated with the development of severe long-term neurological complications such as GBS and congenital microcephaly in newborns (Hayes, 2009) in recent years. This, coupled with the potential of ZIKV to cause another worldwide epidemic has highlighted the need for an effective antiviral against ZIKV. To address the lack of approved antiviral treatments targeted at ZIKV infections, we sought to first identify novel and potent antivirals against ZIKV via a high-throughput screen performed on a 1172-compound FDA-approved drug library. High-throughput screening was done on a phenotype-based screening platform previously developed by our laboratory. The platform utilises an immunofluorescence-based approach on a 96-well format to allow for screening of a large number of small-molecule compounds on human

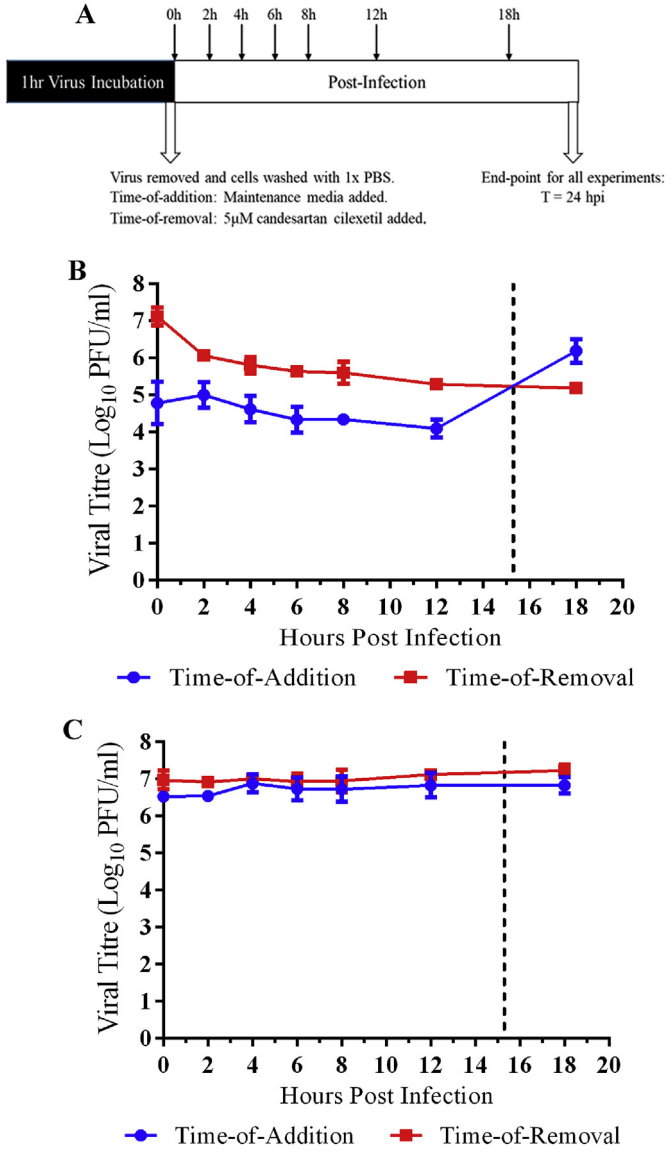

Fig. 4. Time-of-addition and Time-of-removal studies of candesartan cilexetil on ZIKV infection. A) Schematic representation of the approach taken for the time-point dependent studies. B) Time-of-addition and time-of-removal studies. 5 μM candesartan cilexetil was added to or removed from ZIKV-infected JEG-3 cells at specific intervals post-infection. The black line indicates the point of interception, suggesting that candesartan cilexetil exerts its antiviral effect at a post-entry stage(s) of the ZIKV replication cycle. C) ZIKV-infected JEG-3 cells treated with 0.1% DMSO, which served as the positive control for both the time-of-addition and time-of-removal studies. The error bars represent the standard deviation observed from the means of triplicates performed for the time-of-addition and time-of-removal assays.

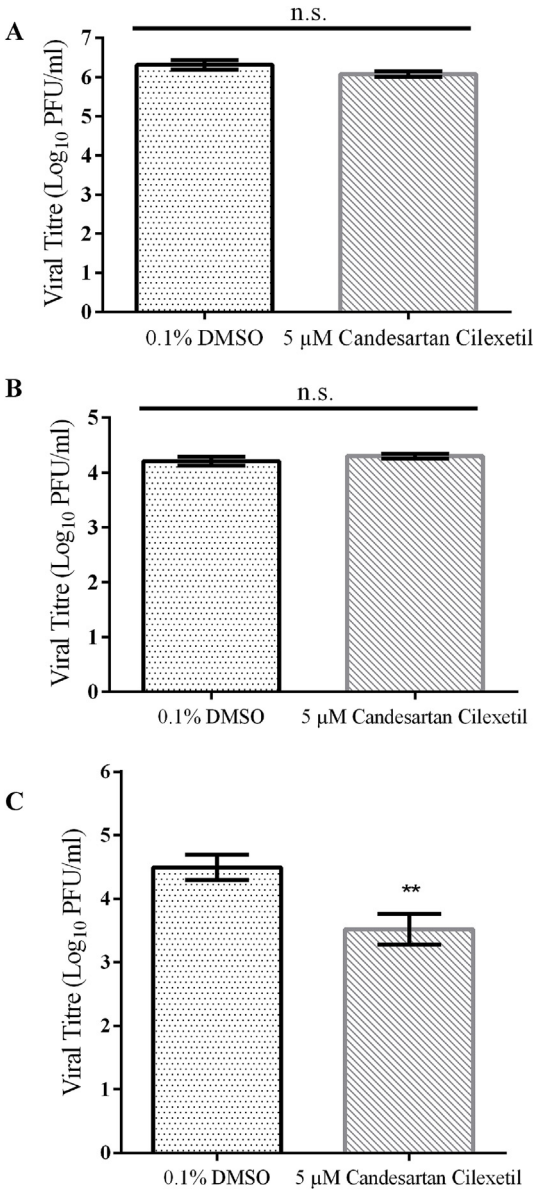

Fig. 5. Pre-treatment, Co-treatment and Entry Bypass studies of candesartan cilexetil on ZIKV infection. A) Pre-treatment of JEG-3 cells with 5 μM candesartan cilexetil failed to significant changes in ZIKV viral titre, indicating that the compound is unlikely to inhibit viral entry into host cells. B) Minimal inhibitory effects were also observed upon co-treatment of ZIKV with 5 μM candesartan cilexetil, suggesting that the compound does not interact with viral surface proteins to inhibit ZIKV infection. C) JEG-3 cells were first transfected with ZIKV viral RNA prior to treatment with candesartan cilexetil. A significant reduction in viral titre was observed upon treatment with the compound, indicating that candesartan cilexetil acts on a post-entry step of the ZIKV replication cycle that likely occurs after the release of the viral genome into the host cell. Two-tailed student's t-test was utilised to determine the presence of any statistical difference. Error bars indicate the standard deviation observed from the means of triplicates that were performed for the pre-treatment, co-treatment and entry bypass studies.

placental JEG-3 cells, enabling rapid identification of compounds with potent antiviral properties. The screening platform was statistically validated and Z-factor value of 0.529 was obtained, indicating that the platform was sufficiently robust and suitable for high-throughput screening. The Z-factor is a simple and dimensionless parameter that is used to establish that the screening platform developed possesses a sufficient dynamic range and an acceptable range of signal variability, which serves to ensure that data generated from the screening platform is useful and accurate (Zhang et al., 1999).

The phenotype-based screening platform was subsequently utilised to conduct a primary screen of the 1172-compound US FDA-approved drug library for potential inhibitors of ZIKV infection. Compounds which yielded ≥50% inhibition of ZIKV infection were classified as positive hits. A total of 29 compounds were identified as positive hits, which included compounds that were also previously reported as hits in a separate screen, namely sorafenib, mercaptopurine, mycophenolate mofetil, mycophenolic, azathioprine and thioguanine (Barrows et al., 2016). In addition, compounds which have been previously reported to express antiviral properties against ZIKV, such as ribavirin (Kamiyama et al., 2017), niclosamide (Xu et al., 2016), gemcitabine (Kuivanen

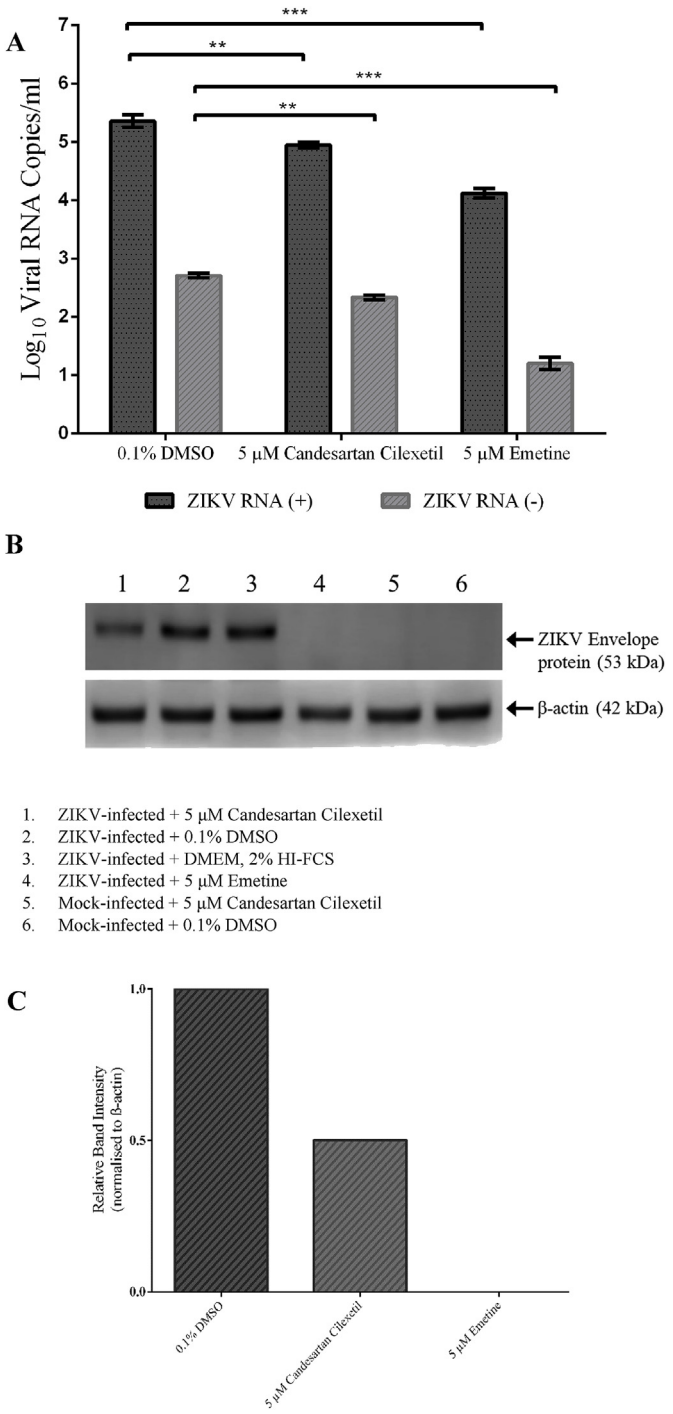

Fig. 6. qRT-PCR and Western Blot analyses of candesartan cilexetil on ZIKV infection. A) Results observed from the qRT-PCR analyses indicate that significant reductions in viral RNA copy numbers for both viral positive- and negative-sense RNA were observed after treatment with 5 μM candesartan cilexetil relative to the vehicle control, 0.1% DMSO. 5 μM emetine served as the positive control. One-way ANOVA and Dunnett's post-test were utilised to determine the presence of any statistical difference, with ** denoting that $P < 0.01$, and *** denoting that $P < 0.001$. Error bars represent the standard deviation observed from the means of triplicates performed for both cell viability and dose-dependent inhibition studies. B) Western blot analyses show a reduction in ZIKV viral protein expression upon treatment with 5 μM candesartan cilexetil relative to the vehicle control, 0.1% DMSO. 5 μM emetine was utilised as the positive control. C) Relative band intensity observed for ZIKV viral envelope protein expression upon treatment with 5 μM candesartan cilexetil, relative to ZIKV viral envelope protein expression upon treatment with 0.1% DMSO.

et al., 2017) and nitazoxanide (Cao et al., 2017) were also amongst the positive hits identified. The presence of these compounds amongst the positive hits identified in the primary screen further validates the reliability of the phenotype-based screening assay used for the identification of potential ZIKV inhibitors. Four compounds were subsequently selected for further validation based on two criteria, the academic novelty of the compound with regards to its antiviral properties and a promising cell viability profile exhibited. The selected compounds were primaquine diphosphate, emetine, calcifediol and candesartan cilexetil.

Dose-dependent inhibition studies were performed for all four compounds to validate and evaluate their anti-ZIKV properties. All four compounds displayed dose-dependent inhibition of ZIKV infection, indicating that these compounds were true positive hits. Amongst the four compounds, candesartan cilexetil exhibited the most potent inhibitory effects against ZIKV at non-cytotoxic concentrations. In JEG-3 cells, the CC_{50} and IC_{50} values of candesartan cilexetil were determined to be 22.33 μM and 3.363 nM respectively, which yielded a selectivity index (SI) value of 6639.9. The antiviral effects of candesartan cilexetil were also investigated in various additional ZIKV-permissible cell lines, with inhibitory effects against ZIKV seen in human embryonic (HEK293T) cells but not in baby hamster kidney (BHK-21) and human hepatoma (Huh7) cell lines. Candesartan cilexetil also demonstrated effectiveness in inhibiting ZIKV infection in human umbilical vein endothelial cells (HUVEC), a primary cell line. In the placenta, the placental barrier cells, which include trophoblasts and endothelial cells play an important role in separating the maternal and fetal blood. Recent studies have also revealed that the HUVEC cell line is permissive for ZIKV infection, enabling it to play a crucial role as a cell model for ZIKV studies (Liu et al., 2016; Richard et al., 2017) This in conjunction with its novel status as an antiviral thus warranted its selection as the lead compound for further downstream investigation into its antiviral mechanism of action.

Candesartan cilexetil is a prodrug that is converted to its active metabolite, candesartan, by esterases in the intestinal wall during absorption from the gastrointestinal tract (McClellan and Goa, 1998). Candesartan is a non-peptide inhibitor of angiotensin II receptor subtype 1 (AT1), which binds selectively to and subsequently dissociates slowly from the receptor. This prevents the binding of angiotensin II, thus blocking its effect (McClellan and Goa, 1998). Candesartan is primarily indicated as a form of treatment for hypertension, however therapeutic effects against congestive heart failure have also been described (Pfeffer et al., 2003).

The antiviral properties of candesartan cilexetil, however, still remains relatively unknown and poorly studied. We thus sought to further elucidate the antiviral mechanism of candesartan cilexetil through a number of secondary assays. Time-of-addition and time-of-removal assays were performed to determine the window period within the ZIKV replication cycle that candesartan cilexetil likely exerts its effect (Kaur et al., 2013). The two curves were observed to intercept at approximately 15.3 h post infection, suggesting that candesartan cilexetil inhibits ZIKV infection at a post-entry stage of the replication cycle. Results from pre-treatment and co-treatment studies also mirrored this observation, as both pre- and co-treatment with candesartan cilexetil failed to yield any significant inhibitory effects on ZIKV, further confirming that the compound does not target the binding and entry steps of the viral replication cycle. These observations were also supported by the results of the subsequent entry bypass study, as candesartan cilexetil was effective in inhibiting ZIKV infection even after direct transfection of JEG-3 cells with ZIKV viral RNA. The effects of candesartan cilexetil on ZIKV RNA replication and protein synthesis were also investigated. Data from qRT-PCR and western blot analyses demonstrated that candesartan cilexetil treatment induced a decrease in the synthesis both positive- and negative sense viral RNA, as well as the viral envelope protein. Taken together, the results obtained from the multiple secondary downstream assays indicate that candesartan cilexetil is acting on a post entry process(es) of the viral replication cycle that occurs

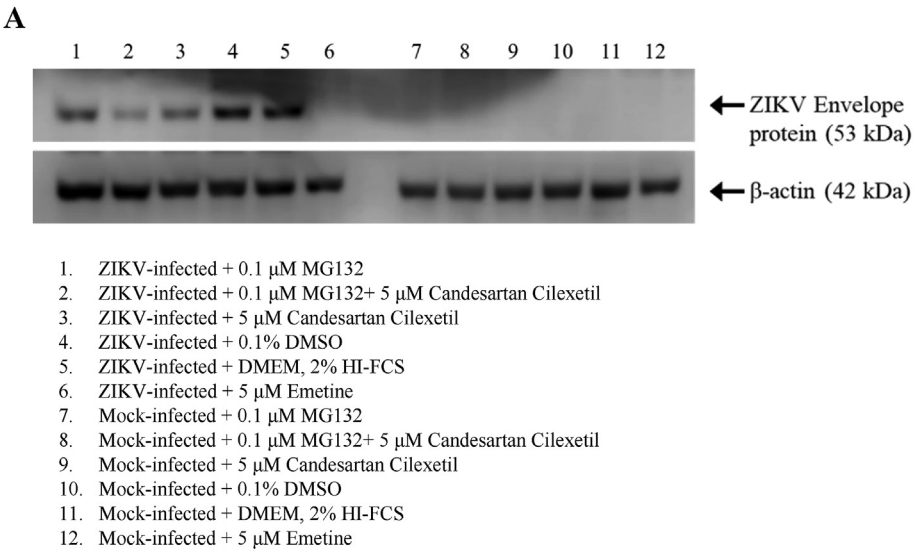

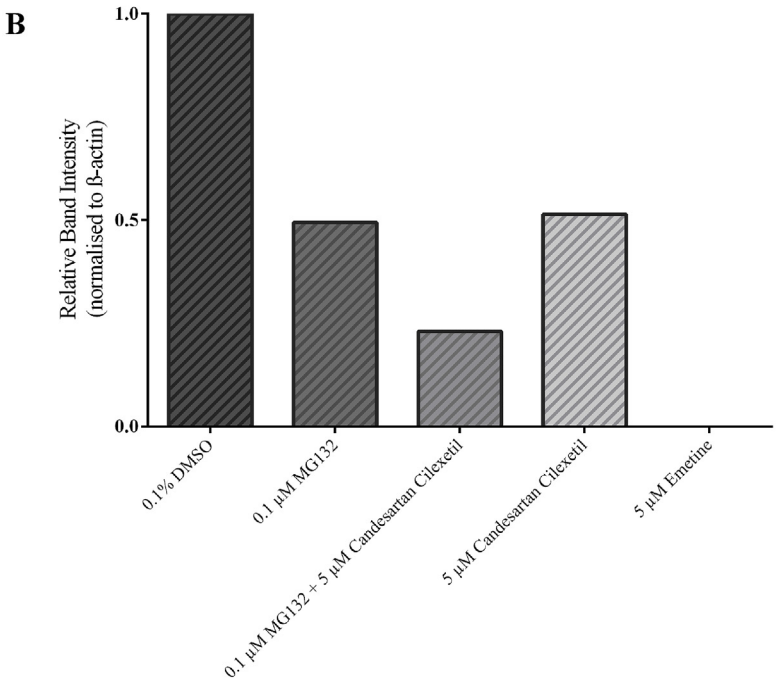

Fig. 7. Western Blot analyses of MG132 in combination with candesartan cilexetil on ZIKV infection. A) Western blot analyses show a reduction in ZIKV viral protein expression relative upon treatment with 0.1 μM in combination with 5 μM candesartan cilexetil relative to the vehicle control, 0.1% DMSO. This observation suggests that the reduction of viral protein expression upon treatment with candesartan cilexetil are unlikely to be mediated via accelerated proteolysis. 5 μM emetine was utilised as the positive control. C) Relative band intensity observed for ZIKV viral envelope protein expression upon treatment with 0.1 μM MG132, 0.1 μM MG132 in combination with 5 μM candesartan cilexetil and 5 μM candesartan cilexetil, relative to ZIKV viral envelope protein expression upon treatment with 0.1% DMSO.

following the release of the viral genome into the host cell cytoplasm.

The effects of candesartan cilexetil treatment on viral protein expression were further investigated, specifically if the observations were potentially due to accelerated proteolysis of the viral proteins. Interestingly, treatment with MG132 induced a further reduction in viral protein levels in the presence of candesartan cilexetil, indicating that the decrease in viral protein expression as a result of candesartan cilexetil treatment is unlikely due to increased proteolysis. As MG132 is a proteosome inhibitor, the addition of the compound likely result in a rescue effect observed for the viral protein expression if the effect of candesartan cilexetil was mediated via accelerated proteolysis. It was also observed that treatment with MG132 alone resulted in a reduction in the expression of the ZIKV viral envelope protein. This has also been reported for various other flaviviruses, such as West Nile virus (WNV) (Fernandez-Garcia et al., 2011; Gilfoy et al., 2009), and Yellow fever virus (YFV) (Fernandez-Garcia et al., 2011). It has been suggested that MG132 inhibits a post-entry step of the flavivirus replication cycle and further investigation via qPCR and the use of a firefly luciferase replicon have indicated that MG132 affects flavivirus RNA replication (Fernandez-Garcia et al., 2011). Given its nature as an RNA virus, the two processes of RNA replication and protein translation are very much interwoven, such that a reduction in one of the process would result in a corresponding impact on the other. Thus, it is unsurprising that treatment with candesartan cilexetil is able to induce an inhibitory effect on both viral RNA replication and viral protein synthesis.

Given that candesartan cilexetil and its active form candesartan acts predominantly via the inhibition of AT_1 receptors, and JEG-3 cells have been reported to express the aforementioned receptors (Nahman et al., 1996; Lanz et al., 2003), it was initially hypothesised that the antiviral properties observed were primarily mediated by the inhibition of AT_1 receptors. However, dose-dependent inhibition studies performed on ZIKV with candesartan have revealed that it does not exhibit any inhibitory effects against ZIKV (Fig. S2). This observation in conjunction with the lack of antiviral properties exhibited by other AT_1 inhibitors such as losartan and irbesartan in the primary screen, has led to the conclusion that the antiviral properties of candesartan cilexetil against ZIKV are likely to be mediated via a different target, instead of via the inhibition of AT_1.

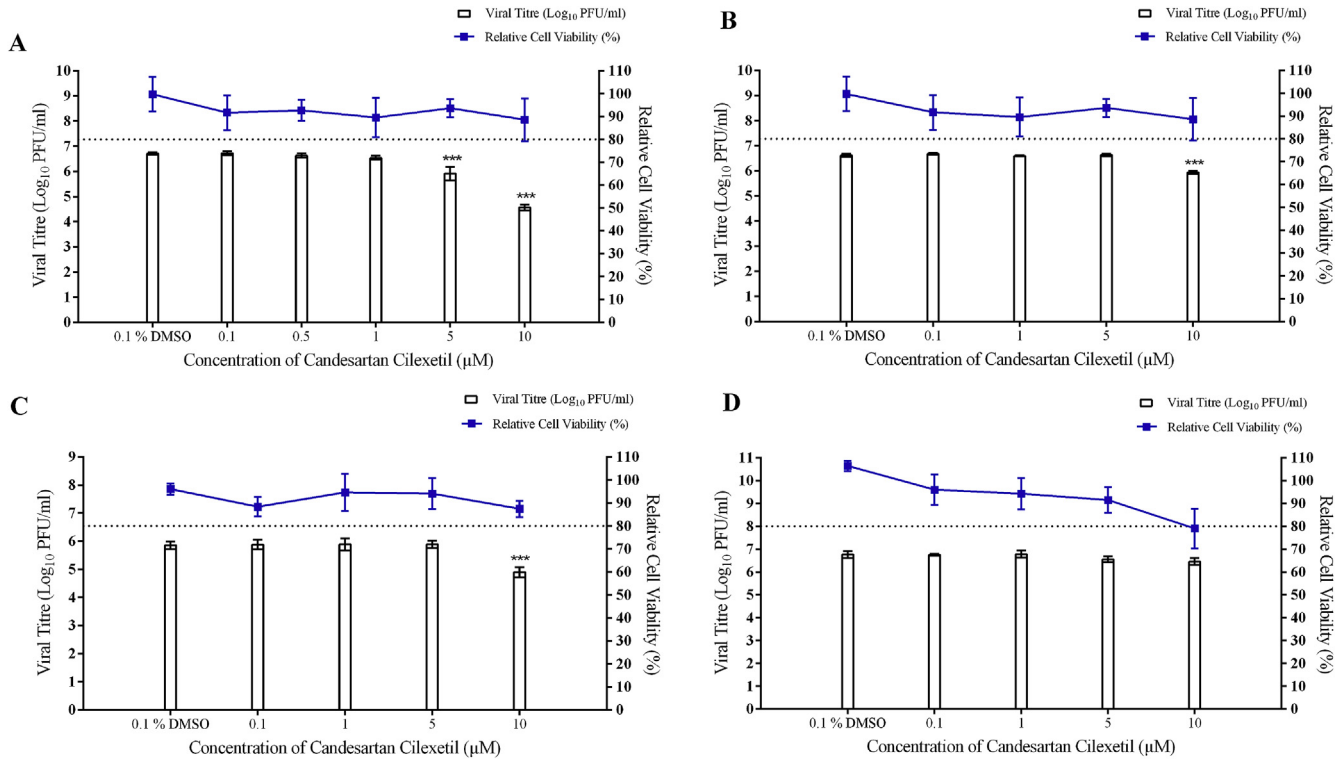

Fig. 8. Antiviral effects of candesartan cilexetil on other viruses. Treatment with candesartan cilexetil was performed on A) DENV2, B) KUNV, C) ECHIKV and D) EV-A71 infected cells, and viral titre quantified via plaque assay. Significant reductions in viral titre were observed for DENV2, KUNV and CHIKV upon treatment with candesartan cilexetil, whereas there was no significant antiviral effects observed against EV-A71. The primary axis corresponds to the viral titre observed, whereas the secondary axis corresponds to the relative cell viability. Dashed line indicates the CC_{20} cut-off for cell viability. One-way ANOVA and Dunnett's post-test were utilised to determine the presence of any statistical difference, with * denoting that $P < 0.05$, and *** denoting that $P < 0.001$. Error bars represent the standard deviation observed from the means of triplicates performed for both cell viability and dose-dependent inhibition studies.

Table 2
IC_{50} values of candesartan cilexetil against ZIKV, DENV2, KUNV and CHIKV.

No.	Virus	Cell Line	IC_{50} (μM)
1	ZIKV	JEG-3	0.003363
2	DENV	HEK293T	1.602
3	KUNV	HEK293T	8.778
4	CHIKV	HeLa	-9.025

To further elucidate its mechanism of action, we attempted to generate and select for resistant mutants against candesartan cilexetil to determine if it acts via the targeting of a viral or host factor (Qing et al., 2010). This was done by repeatedly passaging wild-type ZIKV in presence of increasing concentrations of candesartan cilexetil (Fig. S1A). Treatment with candesartan cilexetil was initially carried out at 4 μM, before being increased to 8 μM from passage 8 onwards. Our results show that viral titre observed for the viruses passaged in candesartan cilexetil initially decreased in the early passages, likely due to the antiviral effects of the compound. However the titre eventually appeared to plateau and eventually increased gradually from passage 5 onwards. At passage 14, viral titre of the candesartan cilexetil-passaged viruses appeared to have reached a similar level to the viruses passaged in 0.1% DMSO and media alone, which served as the controls, suggesting the development of resistance to candesartan cilexetil. Interestingly, further subsequent passages resulted in viral titres observed that were slightly fluctuating, as opposed to a plateau that would be expected for a population of resistant mutants. To further verify the presence of resistant mutants, a dose-dependent inhibition assay was performed with the supernatant harvested from passage 22. However, results observed revealed that the viruses still remained susceptible to treatment with candesartan cilexetil (Fig. S1B). The full genomes of both the wild-type and candesartan cilexetil passaged viruses were also sequenced via next-generation sequencing (NGS), however we did not identify the presence of any differences between the two genomes that could have potentially contributed to resistance against candesartan cilexetil. This may indicate that the compound targets a host factor that is likely to be more resistant to the generation of escape mutants as it potentially has to develop the ability to exploit an alternative host pathway or factor to proceed with the replication cycle, circumventing the inhibition of the host factor by the compound. Additionally, the gradual increase in viral titre seen in turn could be attributed to the attenuation of the virus to JEG-3 cells over the course of multiple successive passages as opposed to the development of drug resistance. Traditionally, antivirals targeting host factors may be advantageous over their direct-acting counterparts which target viral factors in that there is a lower risk of drug resistance emerging via mutations to the viral genome. This is a key area of concern given the nature of ZIKV, as since it is an RNA virus, a distinctive characteristic of its genome replication is the relatively high rate of mutation, which can be predominantly attributed to the absence or low efficacy of proofreading and repair activities that are associated with the enzymes involved, such as the viral replicases, transcriptases and polymerases (Domingo and Holland, 2002). Despite this, further mechanistic studies are still required to evaluate the exact antiviral mechanism of action of candesartan cilexetil.

We also investigated the potential broad-spectrum antiviral properties of candesartan cilexetil against five other viruses, namely DENV2, KUNV, CHIKV and EV-A71. DENV2 and KUNV are closely related to ZIKV, being fellow members of the genus *Flavivirus*, whereas CHIKV and EV-A71 belong to the genera *Alphavirus* (Sreekumar et al., 2010) and *Enterovirus* (Melnick, 1996) respectively. Of the five tested, candesartan cilexetil exhibited significant inhibitory effects against DENV2, KUNV and CHIKV at non-cytotoxic concentrations, indicating that its antiviral

effects is unlikely to be specific to ZIKV and its closely related counterparts. All four viruses, ZIKV, DENV2, KUNV and CHIKV, that candesartan cilexetil demonstrated significant antiviral effects against are arthropod-borne viruses. Additionally, they share similar transmission vectors, as the viruses are all transmitted by members of the mosquito species *Aedes aegypti* and *Aedes albopictus*, with the exception of KUNV, which is predominantly transmitted via the mosquito species *Culex annulirostris*. This, coupled with the similarity in their seasonal correlations and endemic regions have resulted in co-infections of CHIKV, DENV2 and ZIKV becoming an increasingly prominent issue (Rothan et al., 2018). This in turn may indicate that candesartan cilexetil could provide a potential therapeutic avenue for use against these arthropod-borne viruses in the future.

Overall, this study has identified candesartan cilexetil as a novel and potent antiviral against ZIKV infection. Further time-course studies have indicated that it acts on a post-entry stage(s) of the ZIKV replication cycle, and has also demonstrated inhibitory effects against ZIKV viral RNA replication and protein synthesis. Candesartan cilexetil has also shown to exhibit potential broad-spectrum effects against other arthropod-borne viruses. Whilst the potential of candesartan cilexetil as a novel ZIKV antiviral has been highlighted, additional studies are still essential to understand the exact mechanism of its antiviral effects. Furthermore, as the results obtained from this study were from *in vitro* assays, downstream in vivo studies in relevant animal models are still required to assess the efficacy of candesartan cilexetil as an antiviral against ZIKV. A notable contraindication of angiotensin receptor inhibitors such as candesartan is pregnancy due to its well described teratogenic effects such as fetal malformations and neonatal problems that may occur if the drug is administered during pregnancy (Alwan et al., 2005), however it remains to be seen if a similar effect is observed for its pro-drug form. Nevertheless, given the scarcity of antivirals against RNA viruses aside from Human Immunodeficiency Virus (Leyssen et al., 2008), candesartan cilexetil could still potentially serve as a valuable starting point for the developing of novel and potent antivirals in the future.

Acknowledgements

This study was funded by the following grants: MOE Tier 2 grant (MOE 2017-T2-1-078 and MOE 2017-T2-2-014) and Singapore National Research Foundation NRF2016NRF-NSFC002-012.

Appendix A. Supplementary data

Supplementary data to this article can be found online at https://doi.org/10.1016/j.antiviral.2019.104637.

References

Alwan, S., Polifka, J.E., Friedman, J.M., 2005. Angiotensin II receptor antagonist treatment during pregnancy. Birth Defects Res. Part A Clin. Mol. Teratol. https://doi.org/10.1002/bdra.20102.

Araujo, A.Q.C., Silva, M.T.T., Araujo, A.P.Q.C., 2016. Zika virus-associated neurological disorders: a review. Brain 139 (8), 2122–2130. https://doi.org/10.1093/brain/aww158.

Barrows, N.J., Campos, R.K., Powell, S.T., Prasanth, K.R., Schott-Lerner, G., Soto-Acosta, R., et al., 2016. A screen of FDA-approved drugs for inhibitors of zika virus infection. Cell Host Microbe 20 (2), 259–270. https://doi.org/10.1016/j.chom.2016.07.004.

Bullard-Feibelman, K.M., Govero, J., Zhu, Z., Salazar, V., Veselinovic, M., Diamond, M.S., Geiss, B.J., 2017. The FDA-approved drug sofosbuvir inhibits Zika virus infection. Antivir. Res. 137, 134–140. https://doi.org/10.1016/j.antiviral.2016.11.023.

Cao, R.Y., Xu, Y. fen, Zhang, T.H., Yang, J.J., Yuan, Y., Hao, P., et al., 2017. Pediatric drug nitazoxanide: a potential choice for control of Zika. Open Forum Infect. Dis. 4 (1). https://doi.org/10.1093/OFID/OFX009.

Carpenter, A.E., Jones, T.R., Lamprecht, M.R., Clarke, C., Kang, I., Friman, O., ... Sabatini, D.M., 2006. Genome Biol. 7 (10). https://doi.org/10.1186/gb-2006-7-10-r100.

Dick, G.W.A., 1952. Zika Virus (I). Isolations and serological specificity. Trans. R. Soc. Trop. Med. Hyg. 46 (5), 509–520. https://doi.org/10.1016/0035-9203(52)90042-4.

Domingo, E., Holland, J.J., 2002. RNA virus mutations and fitness for survival. Annu. Rev. of Microbiol. https://doi.org/10.1146/annurev.micro.51.1.151.

Faye, O., Freire, C.C.M., Iamarino, A., Faye, O., de Oliveira, J.V.C., Diallo, M., et al., 2014. Molecular evolution of Zika virus during its emergence in the 20(th) century. PLoS Neglected Trop. Dis. 8 (1). https://doi.org/10.1371/journal.pntd.0002636.

Fernandez-Garcia, M.-D., Meertens, L., Bonazzi, M., Cossart, P., Arenzana-Seisdedos, F., Amara, A., 2011. Appraising the roles of CBLL1 and the ubiquitin/proteasome system for flavivirus entry and replication. J. Virol. https://doi.org/10.1128/jvi.02483-10.

Fontes, C.A.P., dos Santos, A.A.S.M.D., Marchiori, E., 2016. Magnetic resonance imaging findings in Guillain-Barré syndrome caused by Zika virus infection. Neuroradiology. https://doi.org/10.1007/s00234-016-1687-9.

Gilfoy, F., Fayzulin, R., Mason, P.W., 2009. West Nile virus genome amplification requires the functional activities of the proteasome. Virology. https://doi.org/10.1016/j.virol.2008.11.034.

Gould, E., Solomon, T., 2008. Pathogenic flaviviruses. The Lancet. https://doi.org/10.1016/S0140-6736(08)60238-X.

Hamel, R., Liégeois, F., Wichit, S., Pompon, J., Diop, F., Talignani, L., et al., 2016. Zika virus: epidemiology, clinical features and host-virus interactions. Microb. Infect. https://doi.org/10.1016/j.micinf.2016.03.009.

Hayes, E.B., 2009. Zika virus outside Africa. Emerg. Infect. Dis. https://doi.org/10.3201/eid1509.090442.

Kamiyama, N., Soma, R., Hidano, S., Watanabe, K., Umekita, H., Fukuda, C., et al., 2017. Ribavirin inhibits Zika virus (ZIKV) replication in vitro and suppresses viremia in ZIKV-infected STAT1-deficient mice. Antivir. Res. 146, 1–11. https://doi.org/10.1016/j.antiviral.2017.08.007.

Kaur, P., Thiruchelvan, M., Lee, R.C.H., Chen, H., Chen, K.C., Ng, M.L., Chu, J.J.H., 2013. Inhibition of Chikungunya virus replication by harringtonine, a novel antiviral that suppresses viral protein expression. Antimicrob. Agents Chemother. 57 (1), 155–167. https://doi.org/10.1128/AAC.01467-12.

Kuivanen, S., Bespalov, M.M., Nandania, J., Ianevski, A., Velagapudi, V., De Brabander, J.K., et al., 2017. Obatoclax, saliphenylhalamide and gemcitabine inhibit Zika virus infection in vitro and differentially affect cellular signaling, transcription and metabolism. Antivir. Res. 139, 117–128. https://doi.org/10.1016/j.antiviral.2016.12.022.

Lanz, B., Kadereit, B., Ernst, S., Shojaati, K., Causevic, M., Frey, B.M., et al., 2003. Angiotensin II regulates 11β-hydroxysteroid dehydrogenase type 2 via AT2 receptors. Kidney Int. https://doi.org/10.1046/j.1523-1755.2003.00192.x.

Lee, J.L., Loe, M.W.C., Lee, R.C.H., Chu, J.J.H., 2019. Antiviral activity of pinocembrin against Zika virus replication. Antivir. Res. 167. https://doi.org/10.1016/j.antiviral.2019.04.003.

Leyssen, P., De Clercq, E., Neyts, J., 2008. Molecular strategies to inhibit the replication of RNA viruses. Antivir. Res. 78 (1), 9–25. https://doi.org/10.1016/j.antiviral.2008.01.004.

Liu, S., Delalio, L.J., Isakson, B.E., Wang, T.T., 2016. AXL-mediated productive infection of human endothelial cells by zika virus. Circ. Res. https://doi.org/10.1161/CIRCRESAHA.116.309866.

Low, J.S., Chen, K.C., Wu, K.X., Ng, M.M., Chu, J.J., 2009. Antiviral activity of emetine dihydrochloride against dengue virus infection. J. Antivir. Antiretrovir. 01 (01), 062–071. https://doi.org/10.4172/jaa.1000009.

McClellan, K.J., Goa, K.L., 1998. Candesartan cilexetil. A review of its use in essential hypertension. Drugs 56 (5), 847–869. Retrieved from. http://www.ncbi.nlm.nih.gov/pubmed/9829158.

Melnick, J.L., 1996. Enteroviruses: polioviruses, coxsackieviruses, echoviruses, and newer enteroviruses. In: Fields, B.N., Knipe, D.M., Howley, P.M., Channock, R.M., Melnick, J.L., Monath, T.P., RoizmanB (Eds.), Straus SE. Fields Virology. Fields Virology.

Musso, D., Gubler, D.J., 2016. Zika virus. Clin. Microbiol. Rev. 29 (3), 487–524. https://doi.org/10.1128/CMR.00072-15.

Musso, D., Nilles, E.J., Cao-Lormeau, V.M., 2014. Rapid spread of emerging Zika virus in the Pacific area. Clin. Microbiol. Infect. 20 (10), O595–O596. https://doi.org/10.1111/1469-0691.12707.

Nahman, N.S., Rothe, K.L., Falkenhain, M.E., Frazer, K.M., Dacio, L.E., Madia, J.D., et al., 1996. Angiotensin II Induction of Fibronectin Biosynthesis in Cultured Human Mesangial Cells: Association with CREB Transcription Factor.

Ong, C.W., 2016. Zika virus: an emerging infectious threat. Intern. Med. J. 46 (5), 525–530. https://doi.org/10.1111/imj.13059.

Pascalino, B.S., Courtemanche, G., Cordeiro, M.T., Gil, L.H.V.G., Freitas-Junior, L., 2016. Zika antiviral chemotherapy: identification of drugs and promising starting points for drug discovery from an FDA-approved library. F1000Research 5, 2523. https://doi.org/10.12688/f1000research.9648.1.

Petersen, L.R., Jamieson, D.J., Powers, A.M., Honein, M.A., 2016. Zika virus. N. Engl. J. Med. https://doi.org/10.1056/NEJMra1602113.

Pfeffer, M.A., Swedberg, K., Granger, C.B., Held, P., McMurray, J.J.V., Michelson, E.L., et al., 2003. Effects of candesartan on mortality and morbidity in patients with chronic heart failure: the CHARM-overall programme. Lancet 362 (9386), 759–766. https://doi.org/10.1016/S0140-6736(03)14282-1.

Qing, M., Zou, G., Wang, Q.Y., Xu, H.Y., Dong, H., Yuan, Z., Shi, P.Y., 2010. Characterization of dengue virus resistance to brequinar in cell culture. Antimicrob. Agents Chemother. https://doi.org/10.1128/AAC.00561-10.

Richard, A.S., Shim, B.-S., Kwon, Y.-C., Zhang, R., Otsuka, Y., Schmitt, K., et al., 2017. AXL-dependent infection of human fetal endothelial cells distinguishes Zika virus from other pathogenic flaviviruses. In: Proceedings of the National Academy of Sciences.

Rothan, H.A., Bidokhti, M.R.M., Byrareddy, S.N., 2018. Current concerns and perspectives on Zika virus co-infection with arboviruses and HIV. J. Autoimmun. https://doi.org/10.1016/j.jaut.2018.01.002.

Saiz, J.C., Martín-Acebes, M.A., 2017. The race to find antivirals for zika virus. Antimicrob. Agents Chemother. 61. https://doi.org/10.1128/AAC.00411-17.

Song, B.H., Yun, S.I., Woolley, M., Lee, Y.M., 2017. Zika virus: history, epidemiology, transmission, and clinical presentation. J. Neuroimmunol. 308, 50–64. https://doi.org/10.1016/j.jneuroim.2017.03.001.

Sreekumar, E., Issac, A., Nair, S., Hariharan, R., Janki, M.B., Arathy, D.S., et al., 2010. Genetic characterization of 2006-2008 isolates of Chikungunya virus from Kerala, South India, by whole genome sequence analysis. Virus Genes. https://doi.org/10.1007/s11262-009-0411-9.

Van Der Hoek, K.H., Eyre, N.S., Shue, B., Khantisitthiporn, O., Glab-Ampi, K., Carr, J.M., Gartner, M.J., Jolly, L.A., Thomas, P.Q., Adikusuma, F., Jankovic-Karasoulos, T., Roberts, C.T., Helbig, K.J., Beard, M.R., 2017. Viperin is an important host restriction factor in control of Zika virus infection. Sci. Rep. 7. https://doi.org/10.1038/s41598-017-04138-1.

WHO | World Health Organization, 2016. WHO statement on the first meeting of the International Health Regulations (2005) (IHR 2005) Emergency Committee on Zika virus and observed increase in neurological disorders and neonatal malformations. WHO 37, 2–5.

World Health Organization, 2018. Zika virus (ZIKV) classification table. https://apps.who.int/iris/bitstream/handle/10665/260419/zika-classification-15Feb18-eng.pdf;jsessionid=F596FE935DD61F93CE78D89457FD3BED?sequence=1.

Xu, M., Lee, E.M., Wen, Z., Cheng, Y., Huang, W.K., Qian, X., et al., 2016. Identification of small-molecule inhibitors of Zika virus infection and induced neural cell death via a drug repurposing screen. Nat. Med. 22 (10), 1101–1107. https://doi.org/10.1038/nm.4184.

Zhang, J.H., Chung, T.D.Y., Oldenburg, K.R., 1999. A Simple Statistical Parameter for Use in Evaluation and Validation of High Throughput Screening Assays. J. Biomol. Screen 4 (2), 67–73. https://doi.org/10.1177/108705719900400206.